A facile hydrothermal recovery of nano sealed MnO_2 particle from waste batteries: An advanced material for electrochemical and environmental applications

M Mylarappa[1, 2], V Venkata Lakshmi[*1], K R Vishnu Mahesh[*3], H P Nagaswarupa[4] and N Raghavendra[5]

[1]Research centre, Department of Chemistry, AMC Engineering College, Bannerghatta Road Bengaluru-560083, Karnataka, India (Affiliated to Tumkur University)
[2]Department of Studies and Research in Chemistry, B.H Road, Tumkur University Tumkur, Karnataka, India
[3]Department of Chemistry, Dayananda Sagar College of Engineering, Bengaluru-78
[4]Research Centre, Department of Chemistry, EWIT, Bengaluru-91
[5]CMRTU, RV College of Campus, Bengaluru-560059

***Email**: [*1] laxmimurthy@rediffmail.com and [*3] vishnumaheshkr@gmail.com*

Abstract: This work deliberates a method for manganese (Mn) recovery as manganese oxide obtained by leaching of waste batteries with 3M sulphuric acid. The Experimental test for the recovery of Mn present within the waste dry cell batteries were carried out by a reductive leachant. Elemental composition of leached sample was confirmed by Energy Dispersive X-ray analysis (EDAX), and Surface morphology of the recovered MnO_2 was examined by using Scanning Electron microscopy (SEM). Phase composition was confirmed from X-ray Diffractro meter (XRD). The obtained leached solution was treated with 4M NaOH, yielded to Manganese Dioxide with high extraction degree, while it do not touches the Zn content within the solutions. The recovered samples were characterized using XRD, EDAX, SEM and Fourier transform infrared spectrometry (FTIR). The electrochemical properties of the as-recovered sample from leached solution was examined used cyclic voltammetry (CV) and electrochemical impedance spectroscopy (EIS). Remarkably, the 80 wt. % MnO_2 displays reversibility, diffusion constant, smaller equivalent series resistance and charge transfer resistance in 0.5M NaOH showed superior results as compared to alternative electrolytes. The ideal capacitive behaviour of MnO_2 electrode and nano particle was applied to photocatalytic degradation of dyes.

Keywords: Battery wastes, Recovery, MnO_2, Electrochemical and photocatalytic applications

1. Introduction

Most of the spent batteries area unit dropped in landfills rather than being recycled and represent a supply of serious metals within the percolate collected at the lowest of the landfill [1-2] and even in underground waters if the landfill isn't adequately protected. Consumed batteries are also burnt in controlled Municipal Solid Waste (MSW)-incinerators beside domestic wastes however fine particles of serious metals may accumulate within the setting owing to the physical state of the electricity filters placed downstream from the burners to forestall escape of solid particles [3]. The consumed batteries area unit utilized in radios, recorders, toys, remote controls, watches, calculators, cameras, and in several different objects. The waste batteries cause a heavy anxiety owing to their poisonousness, abundance and sturdiness within the setting [3]. Area of batteries unit may supplies a valuable metals like Zn and Mn, associated their recovery may represent an Economic profit for the battery producers and reduce to a smaller volume of loss, so prolongation in the lifetime of the landfills. In quitted kind, Zn is present as ZnO, whereas Mn is present as Mn_2O_3 and Mn_3O_4 [1, 4]. To demonstrate the Zn and

Mn substances area unit of 28.3% and 26.3%, separately of the full mass in a particularly waste from dry cell batteries [2]. Such high Zn and Mn substances specify the significance of battery use, each from low-cost and atmosphere views. The hydrometallurgical strategies area unit the foremost common method altogether over the planet as a result of its environmentally appropriate and economical to treat even low Zn and Mn containing materials on tiny scale with high purity and low energy needs [5-6]. Hence, the treatment of those wastes for the recovery of Mn is vigorous for discarded material to staple use. MnO_2 is economic and industrial necessary with applications in several fields like battery business, catalysis, water treatment plants, industry and chemicals. This work is targeted on the extracting of manganese as manganese oxide (MnO_2). This is employed as cathode in consumed batteries that are primarily based within the system Zn/KOH/MnO_2. The initiative of the work reportable here is to improve an electrochemical route for the recovery of Mn as MnO_2 from consumed primary batteries. Experiments were performed to leach out the positive and negative active materials by acid to get chiefly the various components as soluble sulphate. The soluble Mn^{2+} was oxidized to MnO_2 employing a reducer. The studies given within the literature represented the getting of elemental metals, oxides, alloys, salts from spent batteries. Valuable materials may be re-use or synthetize from leach solutions of Spent Batteries (SB). Therefore, Manganese oxides were obtained from SB by chemical methods that were clean, versatile and effective remediation alternative [7]. Among metal oxides, MnO_2 is usually thought-about to be the promising conductor materials for the electro chemical capacitors attributable to its high energy density, low value and environmental friendliness [3].

A major area of study is based on the MnO_2 production and improvement of its electrochemical performance and vital industrial applications like battery trade, water treatment plants, industry and chemicals, during this study shows to recover Mn as MnO_2 from consumed primary batteries employing a hydrometallurgical method, while not purification the concentration of Zn solutions which will be recovered by precipitation or electro winning [8]. The light-converting materials have attracted tremendous attention in recent years for photo catalysis and solar energy collection which can be easily absorbed by given dye and thus effectively excite the dye to generate more electron-hole pairs, resulting in the improvement of the self-sensitized degradation of dye.

The aim of this work is to study the electrochemical and environmental application as photo catalytic performing of MnO_2 using a hydrometallurgical process and the catalytic action of MnO_2 is due to their high efficiency in the reaction/oxidation cycles.

2. Experimental segment

2. 1 Materials and Methods

The waste dry cell batteries were collected from Bengaluru, India at different manufactures. Concentrated H_2SO_4, $H_2C_2O_4$. $2H_2O$ and NaOH of analytical grade were used and they procured from Merck.

2.2. Dissembling and leaching method

The waste dry cell batteries in an amount of 500g were collected from different manufactures. Series of mechanical process is conducted within the following sequence to yield enriched Zn and Mn particles. The waste dry cell batteries were fed to a hammer mill for dismantling. Magnetic extractor removed the magnetic fractions and the non-magnetic fraction were separated in sieve of 2 mm. A second magnetic parting was carried out to eliminate ferrous materials that remains inside the sample. The separated powder was later washed with deionized water to eliminate NH_4Cl electrolyte and potassium within the sample and dried at 373 K for 24 hrs. The washed powder (20 g) was dissolved in 100 mL of 3M H_2SO_4 followed by the addition of 5.94 g oxalic acid dehydrated as leach agent. The leacing was continued for 5 hours at 373 K with continuous stirring and the recovery flow chart for of Mn as MnO_2 as shown in Fig 1.

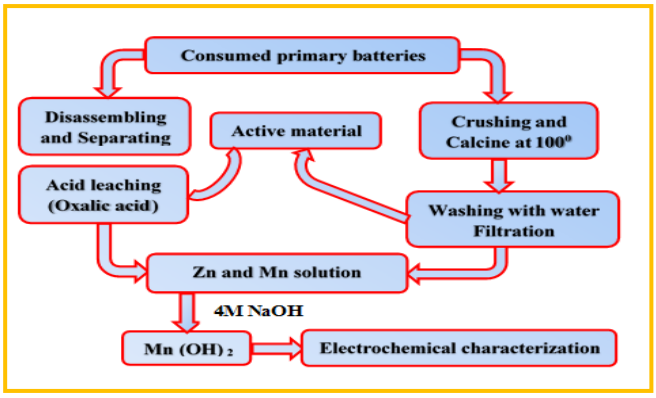

Fig. 1 Flow chart for recovery of Mn from waste dry cell batteries

3. Result and discussion

3.1 Active material characterization

3.1.1 EDAX/SEM and X-ray diffraction analysis

EDAX, SEM and X-ray diffraction analysis were done for active material leaching process with oxalic acid as shown in the Fig. 2 a) and 2 b). EDAX spectra confirmed the Zn and Mn are the most components present in the sample with a trace amount of iron (Fe). The presence of Cl is as a result of NH_4Cl that was used as associate degree solution material in primary batteries. The active powder that was leached oxalic acid (Fig.2 a)) as a chemical agent, clearly shows the expressive quantity of Mn and Zn in the powder. The XRD of active powder leaching with acid from waste dry cell batteries are shown in the Fig.2 b) indicating the presence of manganese oxides (MnO_2, Mn_2O_3, Mn_3O_4) and Zinc oxide (ZnO) were the main constituents [11].

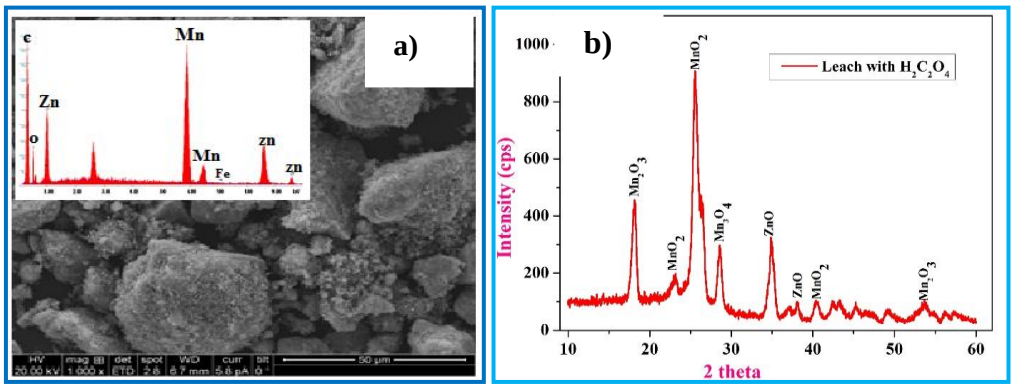

Fig. 2 EDAX, SEM and XRD images of active material leached with 3M oxalic acid

3.2 Extraction of Manganese dioxide from waste Primary batteries

Extraction of Mn as MnO_2 from the leaching solution is feasible at room temperature while not special purification of the solution and conserving a high potency. A required amount of leached solution in a 500 mL beaker and a solution of 4M NaOH was added slowly to the beaker containing leach solution with constant stirring by magnetic stirrer. At the tip of the precipitation, the solution within the beaker was filtered and also the solid residue remained within the filter paper was dried in an oven at 373K for 24 hours. The MnO_2 was fashioned as black precipitate at bottom of the cell. Within the leaching stage, the various compounds of Zn react with H_2SO_4 to provide $ZnSO_4$ and it often understood that there are many different manganese compounds in numerous oxidation state. The reactions of the oxides with the acid provide $MnSO_4$ and MnO_2 as product as shown in Eq. (1) and Eq. (2).

$$Mn_2O_3 + H_2SO_4 \longrightarrow MnSO_4 + MnO_2 + H_2O \quad \ldots\ldots\ldots (1)$$

$$Mn_3O_4 + 2\,H_2SO_4 \longrightarrow 2\,MnSO_4 + MnO_2 + 2\,H_2O \quad \ldots\ldots\ldots (2)$$

The recovered sample were characterized by EDAX, SEM, FTIR and XRD to analyse elemental composition, morphology, functional group and crystallinity of the powder.

3.3 X-Ray diffractometer

X-Ray diffraction were carried out employing a high resolution X-ray Diffractometer Maxima-7000 (Shimandzu) at a scanning rate of 2˚ min^{-1} CuKα radiation (λ = 1.54 Å) operating at 40kV and 30 mA.X-ray diffraction was used to characterize the section and crystal properties of the recovered sample. In Fig. 3, XRD analysis displays that MnO_2, Mn_2O_3 and Mn_3O_4 are the main segments in recovered powder. When treating with 4M NaOH solution, dark precipitate of MnO_2 shows extensive peaks at 2ɵ value at 15.83, 25.3, 35.6 and 62.7 correspond to (0 0 1), (0 0 2) , (100) and (110) planes, that is in smart agreement with the reported patterns for birnessite-type MnO_2 (JCPDS NO.00-018-0802) respectively. No alternative peaks associated with the impurities is found [3, 2, 21]. The section purity of the MnO_2 was examined by XRD. The spectrum of the as-recovered MnO_2 from consumed waste batteries shows an honest variety of great peaks as shown in Fig.3 a). For section determination, this case is common just in case of MnO_2 ready by co-precipitation method [10]. However, the fabric when calcinations showed distinct peaks for the pure section of MnO_2.

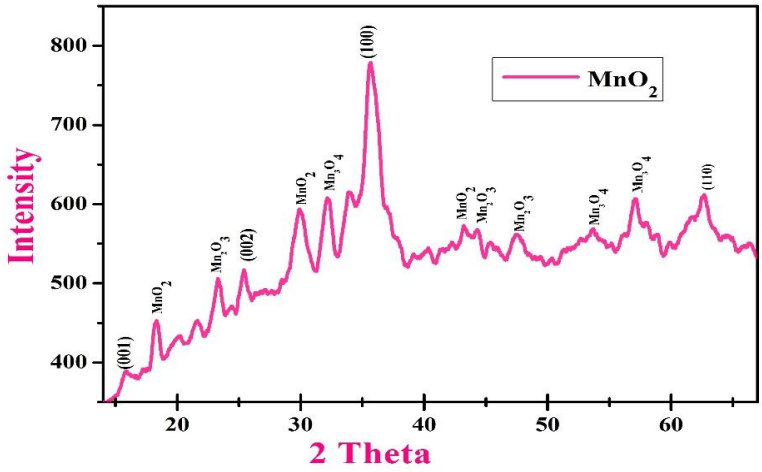

Fig. 3 XRD spectra of extracting MnO_2 from consumed batteries

3.4 EDAX/SEM Analysis

The Energy Dispersive X-ray analysis (EDX) were carried out to get elemental composition of the metals in powder sample. The exact size and morphology of the MnO_2 studied from the Scanning Electronic Microscopy (SEM).In Fig.4 a) to b), shows that manganese and oxygen contents were detected in the spectrum, indicating the presence of expressive content of manganese hydroxide [6].The leaching residue showed virtually similar particle size compared to it before leaching. Particles area unit well distributed throughout with showing less agglomerations and particle size ranges from 5 to 30 µm. EDX of the leaching residue indicated that it contain unleachable Mn species that was attributed to a metal oxide species ensuing from the initial cell materials [7].

In Fig.4 a) shows a typical SEM image of MnO_2 with the diameter concerning 20 µm having a stratified porous structure that's shaped by the self-assembly of MnO_2 platelets, i.e.in good agreement with the results of XRD by the self-assembly of MnO_2 platelets, that is in good agreement with the results of XRD and FTIR spectra [2]. In Fig.4, clearly seen that the Mn_2O_3 and Mn_3O_4 particles are randomly scattered in dried active powder with asymmetrical sizes and shapes. The SEM image of MnO_2 spheres (Fig.4 b) shows that the majority particles are uniform and spherical with a diameter of around 20 µm.

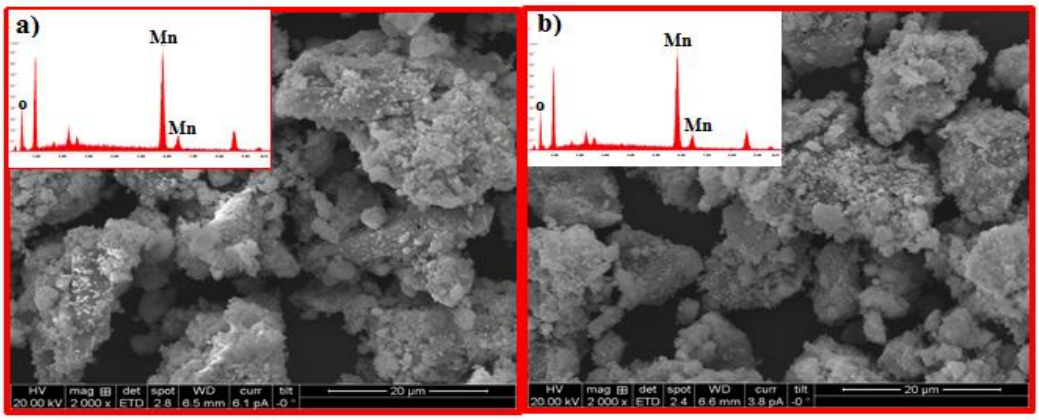

Fig.4 EDAX/SEM images of Recovered MnO_2 a) Calcine at 373 K b) calcine at 473 K

3.5 Fourier transform infrared spectra

The FTIR spectrum of MnO_2 within the wavenumber vary from 400-4000 cm^{-1} as shown in Fig. 5 a) to c). The peak at some 538 cm^{-1}, that is ascribed to the Mn-O bond, seems and becomes more and more intense [1-2]. The strong absorption band at 538 cm^{-1} can be allotted to the Mn-O stretching mode, demonstrating the existence of Mn-O bond among MnO_2 structure. The absorption bands at 1356.62 cm^{-1}, 1172.25 cm^{-1}, 1165.95 cm^{-1} and 1046.9 cm^{-1} match to the O-H bending vibrations joined with Mn atoms, whereas the absorption band at 2081 cm^{-1} arise due to completely different degree of hydrogen bonding within the sample. The observation of O-H vibrations in FTIR spectrum suggests the presence of absorbed water molecules among MnO_2 structure. The hydrated properties of MnO_2 might enrich the cations diffusion thereby increasing capacitance of MnO_2 [3, 10].

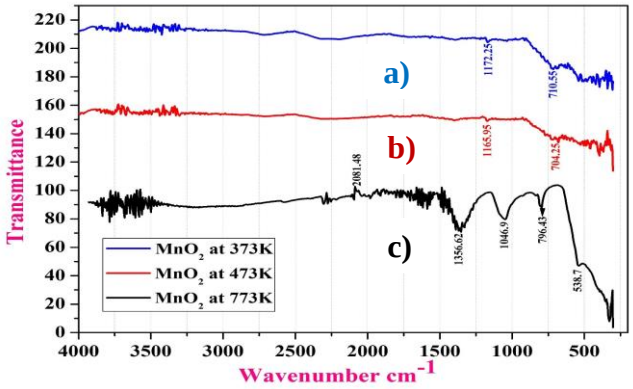

Fig. 5 FTIR spectrum of MnO_2

4. Electrochemical Characterization

4.1 Cyclic Voltammetry Studies

The MnO_2 electrode was prepared by the mixture of 80 wt. % of MnO_2 powder as active material with 20 wt. % of graphite and silicone oil used as binder. The constituents were well mixed to get the uniform composition. Electrochemical activity of MnO_2 was assessed by cyclic voltammetry (CV). An electrochemical measurements involves three electrode system having working, Ag/AgCl reference electrode and a platinum wire as counter electrode. The CV studies were performed in potential between 0 to -1 V using 0.5M KCl, 0.5M Na_2SO_4, 0.5M NaCl and 0.5M NaOH electrolytes at constant scan rate [9,11]. To evaluate the electrochemical reversibility (ER) of the sample, the potential window of CV was modified from 0 to -1 V and sweep rate 10 mV as shown in Fig. 6 a) and the influence of scan rate is accessible for different electrolytes as shown in Fig.6 b) to e). As the scan rate

rises, the CV side view differs from the ideal capacitive performance. This is generally because of the redox reactions depend on the insertion - deinsertion of the protons from the electrolyte .At slow scan rates, the dispersion of ions from the electrolyte can upgrading access to just about all presented pores on the electrode surface, leading to a whole insertion reaction. In general an estimate of the reversible potential difference between the anodic (E_a) and cathodic (E_c) peak potential were determined by the reversibility of the redox reaction [20-21]. The comparative CV results of electrode in several electrolytes at scan rate of 10 mVs^{-1} are tabulated in Table 1. The experimental information shows the redox reactions for all electrolytes as indicating by the moderately large E_a-E_c. But the E_a-E_c of electrode in 0.5M NaOH is merely 0.0332mV that is smaller than that of different electrolytes as seen in the Table.1. This indicates the charge discharge method of the electrode in 0.5M NaOH shows superior reversibility than different electrolytes. It will recognises the electrochemical reaction of a given electrode is restricted by proton diffusion through the lattice [22]. Therefore it is necessary to check MnO_2 electrode proton diffusion coefficient. According to the Randlese sevcik equation [22], the peak current is depicted by as shown in Eq. (3) and Eq. (4)

$$\mathbf{i_p = 2.69 \times 10^5 \times n^{3/2} \times A \times D^{1/2} \times C_o \times V^{1/2}} \quad \ldots\ldots\ldots \quad (3)$$

Where n ⟶ electron number of the reaction
A ⟶ surface area of the electrode
D ⟶ diffusion coefficient
V ⟶ scan rate
C_o ⟶ initial concentration of the reactant

For the MnO_2 electrode, $\mathbf{Co = \rho / M}$ ……. (4)

Where the theoretical density of MnO_2 electrode and its molar mass are represented by ρ and M respectively. From equation (3), for sample MnO_2 in 0.5M NaOH solution, the proton diffusion coefficient is calculated to be 2.1990×10^{-5} cm^2/s which is larger as compared to that of other electrolytes.

Table 1. Potential values of CV characteristic for different electrolytes.

Electrolytes	E_a(mv)	E_c(mv)	E_a-E_c	$D \times 10^{-5}$(cm^2/s)
0.5M KCl	0.3385	0.3053	0.0332	0.9731
0.5M Na_2SO_4	0.6509	0.1245	0.0526	0.5668
0.5M NaOH	0.7677	0.2873	0.4784	2.1990
0.5M NaCl	0.5919	0.3348	0.2571	0.8393

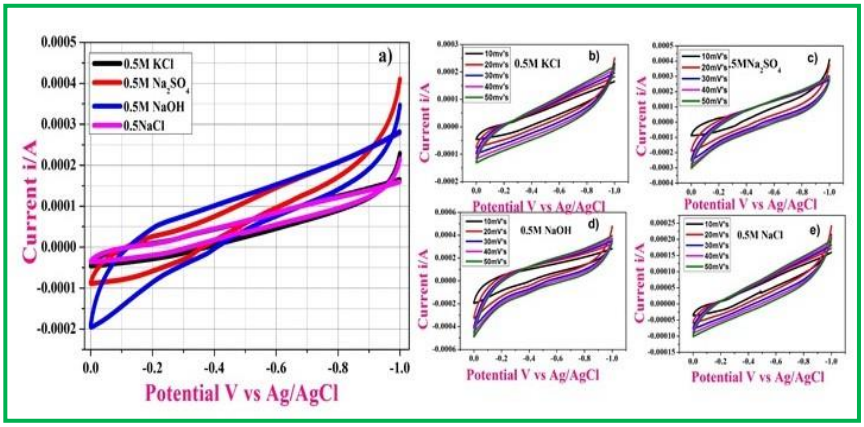

Fig. 6 cyclic voltammograms of MnO_2 electrode using different electrolytes at 10mV/s sweep rate and different sweep rates.

4.2 Electrochemical Impedance Spectra

The electrochemical impedance spectra (EIS) studies were performed to evaluate the electrochemical properties of MnO_2 electrode. Typical Nyquist plots of EIS for electrode as shown in Fig.7 a) to e). Within the equivalent circuit, the symbols Rs, Rct, C, W, Q were denotes the solution resistance, charge-transfer resistance, double layer capacitance, Warburg impedance, and phase constant, respectively. All the EIS spectra were combination of an estimated semicircle in high frequencies and a line in low frequencies [14]. In Fig.7, the low frequency region, the resistance will increase sharply and tends to become vertical lines [1]. At the high frequencies, it's seeming that the values of Rs and Rct bit by bit reduce with reducing MnO_2 loading. At a low scan rate of 5, 10 and 50 mVs^{-1}, shows the estimated rectangular resemblance characteristic of capacitive behaviour [15-17] and a little contact resistance. The EIS information is analysed with Nyquist plot. It shows that the frequency response at the electrode/electrolyte system is an outline of imaginary component (-Z') of the impedance against the real component (Z"). The Nyquist plot of MnO_2 electrode (Fig.7) options a semicircle at high frequencies followed by a near to vertical line at low frequencies. The joining of coordinate axis denotes the majority of solution resistance, comprising of electrolyte resistance, intrinsic resistance of substrate and a solution resistance between active material and current collector [3]. The nearer to vertical line at low frequencies shows that the supreme capacitive behaviour of MnO_2 electrode, indicating the potential of MnO_2 recovered from waste battery within the application of quick charge/discharge for supercapacitors [18].

Table 2. Charge transfer resistance and capacitance of electrode.

Electrolytes	Rct(ohm)	C(F)×10^{-5}
0.5M KCl	21.29	0.01274
0.5M Na_2SO_4	12.1	0.02385
0.5M NaOH	11.96	3.9906
0.5M NaCl	11.77	0.52172

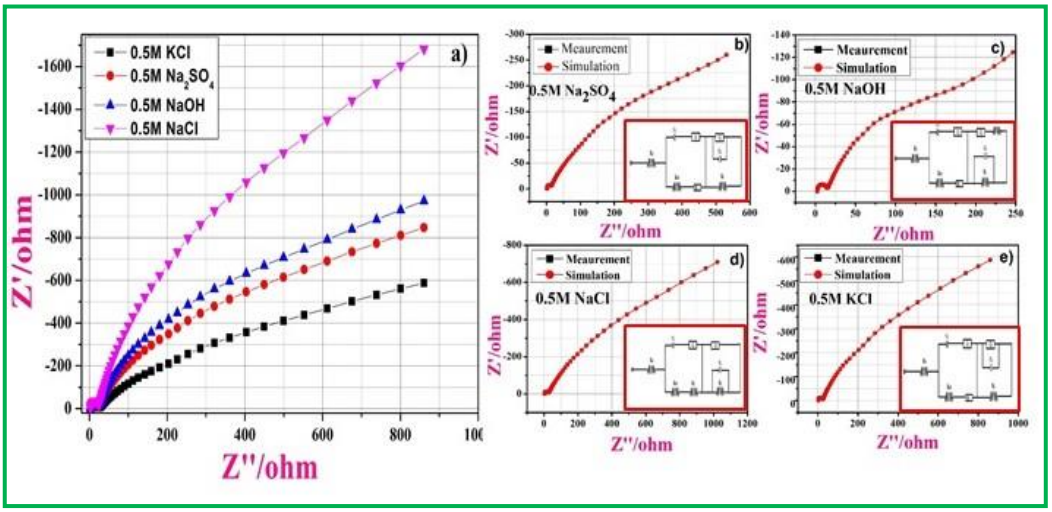

Fig. 7 Nyquist plots of MnO_2 Electrode at different electrolytes with equivalent circuits.

4.3 Photocatalytic Activity of MnO_2

The photocatalytic enactment of the as-prepared sample was assessed through the photocatalytic degradation of Indigo carmine(IC), methyl orange (MO) and malachite green (MG) under visible light irradiation. 0.06 g of MnO_2 was dispersed in 250 ml IC (20ppm) and similarly MO and MG aqueous solutions respectively. The mixed suspensions were first magnetically stirred for 30 min to reach the adsorption-desorption equilibrium. Under the ambient conditions and stirring, the mixed suspensions

were exposed to visible light irradiation produced by a 400W metal Philips lamp (wavelength: 254 nm). At certain time intervals, 5 ml of the mixed suspensions was extracted. The filtrates were analysed by recording UV-vis spectra of IC, MO and MG using a Spectratreats 3.11.01 Release 2A UV-vis spectrophotometer.The UV-Vis absorption of MnO_2 show an intense absorption band in the range 200 to 220 nm. In Fig. 8 shows the UV-vis absorption spectra of IC, MO and MG as a function of the catalytic reaction time. Both IC, MO and MG solutions were turns colorless after 60 min that indicates that complete degradation of dye molecules by MnO_2 showed a better catalytic degradation. It is indicated that the as recovered material, the MO solution with concentration 0.06 g/L can be degraded up to 65.16 % in 60 minutes compared to that of other dyes.

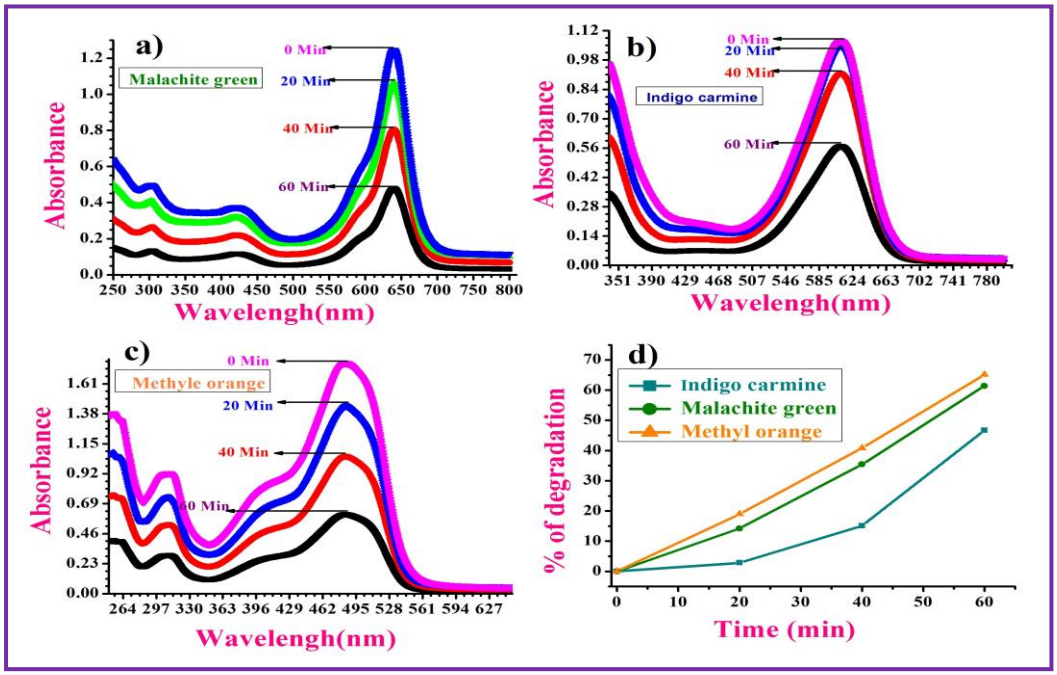

Fig.8 UV-vis absorption spectra of RB and IC as role of time catalysed by MnO_2

Table 3. Percentage degradation of dyes.

Sl No	Name of dye	% of degradation
1	Indigo carmine	46.68
2	Malachite green	61.396
3	Methyl orange	65.16

5. Conclusion

MnO_2 was succefully recovered from battery waste by the mixture of leaching and precipitation method. CV shows that MnO_2 possess good capacitive behaviour. Electrochemical performance suggested that the CV curves of MnO_2-80 wt. % active material at different scan rates in several electrolytes showed reversibility, diffusion coefficient and ideal capacitive behaviours with rectangular-like form in 0.5 M NaOH is best compared to that of other electrolytes. The recovered sample at, 373 K, 20 % oxalic acid and 5 hrs provide high electrochemical activity when the precipitates are kept at 773 K for 1 hr. The electrical capability of this sample in 0.5M NaOH showed a high performance as compared with the other electrolytes. It was showed that as recovered MnO_2, the MO solution with concentration 0.06 g/L can be degraded up to 65.16 % in 60 minutes compared to that of other dyes. The overall results represented that the chemical oxidization of Mn from waste

batteries activity with oxalic acid is an appropriate technique for Mn recovery as MnO_2, it could be utilized for recycling of the spent batteries.

Acknowledgment:
The one of the author (Mylarappa.M) thank to the management and Principal of SJRC for their encouragement in extending the lab facilities and also thankful to Principal and management of East West Institute of Technology for completion of the work.

References

[1] Karnchanawong S, Limpiteeprakan P, *Waste Manag*. 29, 2009 **550**- 558.
[2] Xara S.M, Delgado J.N, Almeida M.F, Costa C.A, *Waste Manag.* 29, 2009, **2121**-2131.
[3] Belardi G, Ballirano P, Ferrini M, Lavecchia R, Medici F, Piga L, Scoppettuolo A, *Thermochem. Acta*. 526, 2011, **169**-177.
[4] U.S. Geological Survey, Mineral Commodity Summaries, January 2009.
[5] Agnieszka, Sobianowska, Turek, Włodzimierz, Szczepaniak, Monika, Zabłocka, Malicka, *J. Power Sources*. 270, 2014**, 668**-674.
[6] Baba A.A, Adekola A.F, Bale R.B, *J. power sources.* 2009, 171, **838**-844.
[7] Paola Macolino, Adriana Loredana Manciulea, Ida De Michelis, Muresan Silviu Anton, Petru Ilea, Francesco Veglio, *Acta Metallur. Slovaca*. 19, 2013, **212**-222.
[8] Maria V, Gallegos, Lorena R, Falco, A, Miguel, Peluso, Jorge E, Sambeth, Horacio J, Thomas, *Waste Manage.* 33 2013, **1483**-1490.
[9] Aleksandra Gonciaruk, Khalid Althumayri, Wayne J, Harrison, Peter M, Budd, Flor Siperstein R, *Micro and Meso Mater*. 209, 2015, **126**-134.
[10] Sait Kursunoglu, Muammer, Kavya, Physicochemical, *Probl. Miner Process*. 50, 2014, **39**-53.
[11] SiXu Deng, Dan Sun, ChunHui Wu, Hao Wang, JingBing Liu, YuXiu Sun, Hui Yan, *Electrochem. Acta.* 111, 2013, **707**-712.
[12] Chen P.C, Shen G.Z, Shi Y, Chen H.T, Zhou C.W, *ACS Nano.* 4, 2010, **4403**.
[13] Di Fabio A, Giorgi A, Mastragostino M, Soavi F, Carbon-poly (3-methylthiophene). *Electrochemical Society*.
[14] Reddy R.N, Reddy R.G, *J. Power Sources.* 124, 2003, **330**-337.
[15] Cheng Q, Tang J, Ma J, Zhang H, Shinya N, Qin L.C, *Carbon* 49, 2011, **2917**-2925.
[16] Liu Y, Yan D, Zhuo R.F, Li S.K, Wu Z.G, Wang J, Ren P.Y, Yan P.X, Geng Z.R, *J. Power Sources.* 242, 2013, **78**.
[17] Freitas M.B.J.G, Pegoretti V.C, Pietre M.K, *J. Power Sources*. 164, 2007, **947**.
[18] Zhang W.G, Jiang W.Q, Yu L.M, Fu Z.Z, Xia W and Yang M.L, *Int.J.Hydrogen Energy*. 34, 2009, **473**.
[19] Bing L, Huatang Y, Yunshi Z, Zuoxing Z and Deying S, J. *Power sources.* 79, 1999, **277**.
[20] Zimmerman H A and P.K, Effa J, *Electrochem.Sci*.131, 1984,**709**.
[21] Rácz R, Ilea P, *Hydrometall.* 2013.
[22] Ravi Kumar C.R, Kotteswaran P, Santosh M.S, Shruthi B, Shivakumara M.S and Nagaswarupa H.P, *Asian Journal of Chemistry* 2015, **221**-229.
[23] Chanhlin Yu, Gao Li, Longfu Wei, Qizhe Fan, Qing Shu, Jimmy C.Yu, *Catalysis Today*, 224, 2014, **154**-162.
[24] Yuqian Li, Jiangying Qu, Feng Gao, Siyuan Lv, Lin Shi, Chunxiang He ,Jingchang Sun, *Appl. Catalysis B: Environ.* 162, 2015, **68**-274
[25] Khalid Abdelazez Mohamed Ahmed, Hong Peng, Kangbing Wu, Kaixun Huang, *Chem. Engg. J.*172, 2011, **531**-539